Scientific Journal of Silesian University of Technology. Series Transport
Zeszyty Naukowe Politechniki Śląskiej. Seria Transport

Volume 116 **2022**

p-ISSN: 0209-3324

e-ISSN: 2450-1549

DOI: https://doi.org/10.20858/sjsutst.2022.116.17

Journal homepage: http://sjsutst.polsl.pl

Article citation information:
Wheatley G., Zaeimi M. Anti-roll bar design for a Formula SAE vehicle suspension. *Scientific Journal of Silesian University of Technology. Series Transport*. 2022, **116**, 257-270. ISSN: 0209-3324. DOI: https://doi.org/10.20858/sjsutst.2022.116.17.

Greg WHEATLEY[1], Mohammad ZAEIMI[2]

ANTI-ROLL BAR DESIGN FOR A FORMULA SAE VEHICLE SUSPENSION

Summary. This work outlines the development and analysis of an anti-roll bar system vehicle carried out by James Cook University. A detailed design phase was completed, clearly showing all stages of the design approach from the initial proposed design to the final design. Several analysis strategies are used throughout the report including weld calculations and FEA modelling. These calculations led to design changes impacting the final recommended system. This report demonstrates compliance with all Formula SAE rules regarding anti-roll bar systems.

Keywords: anti-roll bar system, finite element analysis, Formula SAE, suspension system

1. INTRODUCTION

Although anti-roll bar (ARB) systems have a simple function, their design is influenced by many factors which are not often precisely known including available space, materials, vehicle weight transfer, roll resistance, vehicle and suspension and geometry. Therefore, some assumptions should be made during the design process. Calculations assume a totally rigid

[1] College of Science and Engineering, James Cook University, Townsville, Australia.
Email: greg.wheatley@jcu.edu.au. ORCID: https://orcid.org/0000-0001-9416-3908
[2] Mechanical Engineering Department, University of Guilan, Rasht, Iran.
Email: mohammad.zaeimi@gmail.com. ORCID: https://orcid.org/0000-0003-0987-9253

chassis, friction-free mountings, geometric perfection, symmetric weight distribution on a stationary car, no flexing of ARB levers and steady-state cornering conditions [1]. The impossibility of obtaining and designing for all of these parameters necessitates the use of track testing to finalize the design and emphasizes the difficulty of obtaining an accurate design based on purely theoretical calculations [2]. Materials have also been developed significantly to optimize the strength to weight ratio. Originating from a steel tube or rod bent between 50 and 90 degrees [1], ARBs have been developed into multi-component devices with materials such as Teflon, aluminium, high strength steels and composites such as carbon fibre.

University Racing Eindhoven (URE) [3], proposed a design involving a solid ARB with splined ends and carbon fibre drop rods with aluminium inserts. The levers were welded to a splined bushing, which slid over the ends of the bar and was axially fixed by a c-clip. URE's method highlights the important parameters in the ARB system design. Their results are used for comparison in this study. This project aims to develop a front and rear ARB system with mechanically adjustable system settings. Adjustment settings must be easily accessible for fast changes without the removal of other major components. The recommended design must also comply with all relevant rules and regulations of the FSAE competition [4].

2. DESIGN APPROACH

ARBs are characterized by their torsional resistance. If the stiffness is too soft, the ARB provides limited roll resistance and the vehicle has a greater tendency to oversteer or understeer. Conversely, if the ARB is too hard, it reduces vehicle turnability and may cause the tyre to skip along the road surface. Excessive oversteer or a need to increase understeer can be achieved by slackening the rear ARB or increasing the stiffness of the front ARB [5]. The opposite configuration is used to address excessive understeer.

2.1. Preliminary considerations

Rules and regulations from the Australian Formula SAE [4] are considered in the design of the ARB. The geometry of the ARB is dependent on the location of the mounting points and the range of movements of the suspension system. First, the ARB is to be located in an area with sufficient space, both for the rotation of the lever arms and easy access to the adjustment settings. Second, it has to be mounted to a solid bar that is not subject to flexing during vehicle cornering. This will most likely be a member of the frame that is parallel to the axis of suspension. Next, the position of the ARBs must be close to the suspension system. A remote linkage connecting the ARBs to the suspension may prove unreliable, and therefore, will not be considered. Finally, the front and rear ARBs must be positioned such that the stiffness settings can be easily adjusted without the removal of other major vehicle components. Furthermore, the geometry of the rockers is highly influential on the function of the bar, where the rotation of the rockers determines the displacement of the end of the ARB lever arms. Heim joints are placed between the two parallel faces of each rocker and threaded into the drop link rods. The distance between the parallel faces determines the size of the spacers to be used on either side of the heim joint head but do not present significant constraints regarding the heim joint size.

Due to the varying load application, the material is required to provide sufficient fatigue life. Sharp geometric discontinuities are to be avoided, if possible, to reduce areas of high stress concentration. The chosen material must also satisfy the manufacturing criteria. Aluminium has

the high strength-to-weight ratio desired in the motorsports industry but is expensive and has low weldability. Aluminium welding operations require a tungsten inert gas welder, and due to the melting properties of aluminium, it can be very difficult to work with if not properly experienced. Unlike aluminium, steel has good strength properties and is easily welded; however, it is heavier. Furthermore, Chromoly (4130 Steel–Chrome Molybdenum) was an option which was considered the possibility of its use. The high strength-to-weight ratio makes Chromoly desirable for different applications.

2.2. Initial design

The first concept of the ARB is shown in Figure 1. There are two options available for the bar, tubular or solid rod. Tubular ARBs have a weight/stiffness ratio advantage over solid metal but can cause welding difficulties if chosen as the lever arm connection choice. Solid bars are stronger and have greater torsional stiffness compared to tubes; however, they have a greater sensitivity to outside diameter alterations than tubes [1]. The initial design was on a tube due to its strength-to-weight ratio advantage.

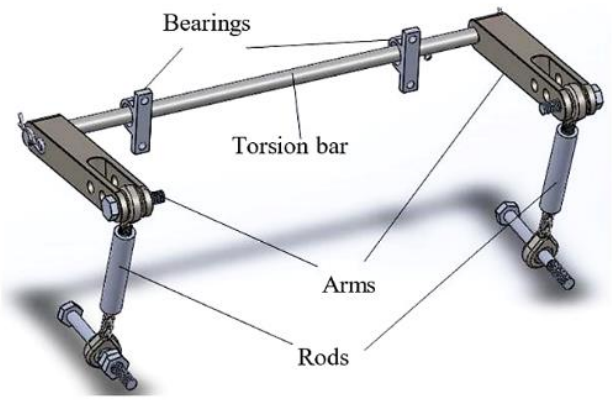

Fig. 1. First design of the anti-roll bar

One considerable concern is with the connection between the lever arms and the bar. The connection between the lever arms and the main bar can be a keyway that drives torsion to the bar, and a clip to prevent sliding, as shown in Figure 2a. Keyways are often used to transfer torque through components such as is used in the rear hub shaft of the current FSAE vehicle. The main disadvantage of using keyways in ARBs is that a precision machining is required to ensure that the fitting clearance is below the required tolerance, which can be both complex and costly. Although it is not anticipated that the bar will be subjected to significant longitudinal loads, the clip may not provide sufficient security and may fall off or loosen during racing conditions.

Another option is to minimize the clearance in the joint between the lever arms and the bar. For this purpose, a hexagon shaped end of the bar was suggested. This end slot in a hexagonal hole through the lever arms is shown in Figure 2b. In this way, the force would be divided up consistently on any edge of the hexagon instead of just on the keyway. The assembly could be locked with a special retaining ring fitted in a rut on the hexagonal end. These rings are cheap and are specially made for such a purpose. The chance of losing this retaining ring is greatly reduced as opposed to the simple clip used in the previous design. However, the major flaw of

this design is the manufacturing difficulty to produce the complex shape hole and bar end. Manufacturing process would require CNC machining, which is costly. In addition, this option also requires a solid bar, which has a weight/stiffness ratio disadvantage compared to tubes. In consideration of this, the design progressed to welded joints.

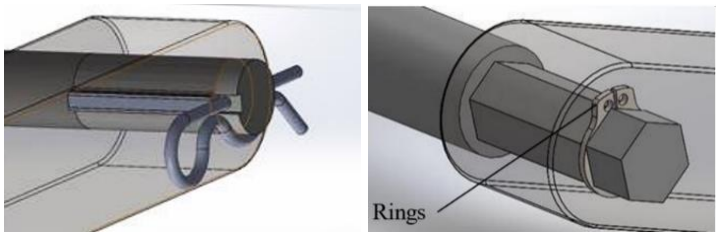

(a) (b)

Fig. 2. Lever arm connection by; (a) keyway, (b) minimizing the clearance in the joint

Another concern was related to the material and geometry of the lever arms. They can be made of steel and thick enough to encompass the rod. As shown in Figure 3a, there are 3 adjustment slots that can apply the most torque to the ARB through a greater moment arm. To simplify the entire design and reduce manufacturing costs, the lever arms were divided up into flat sheets instead of one thick block (Figure 3b). An advantage of this solution is the weight reduction and stiffer arms. This results in less bending in the arms and almost all of the height difference between the arms while cornering is caused by the torsion of the bar. These sheets will be fixed in parallel planes at specific distance apart and welded to the round bar. For optimized force translation and weight reduction, the height of the sheet decreases over its length.

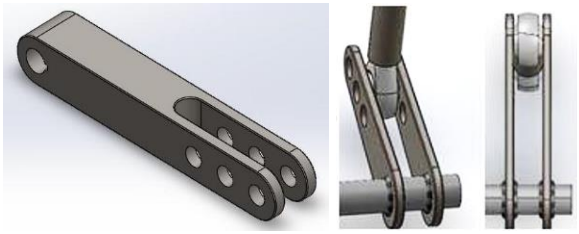

(a) (b)

Fig. 3. Lever arm; (a) thick block, (b) flat sheets

Since the method for joining the lever arms to the bar is welding, this allows the lever arms to be set at any angle and is easier and cheaper to manufacture. A problem with interfacing the tube design decision with the welding proposal is depending on the wall thickness of the tube, as it could be difficult to weld the arms on the tube if there is not enough material. For this situation, some solid steel will be welded into the tube at the sections where the arms will be welded (Figure 4a). The vertical rods used in the design consist of three components; two heim joints threaded into a solid bar that was drilled at tapped either end, as presented in Figure 4b. This design would provide strength and resilience against bending stress. The heim joints were fixed to the lever arms and rockers via hex bolts. The heim joints ensured that the rod could be arranged at different angles to vary the lever arm length and apply different torsions to the ARB.

(a) (b)

Fig. 4. (a) Welded-in material, (b) Vertical rod with heim joints

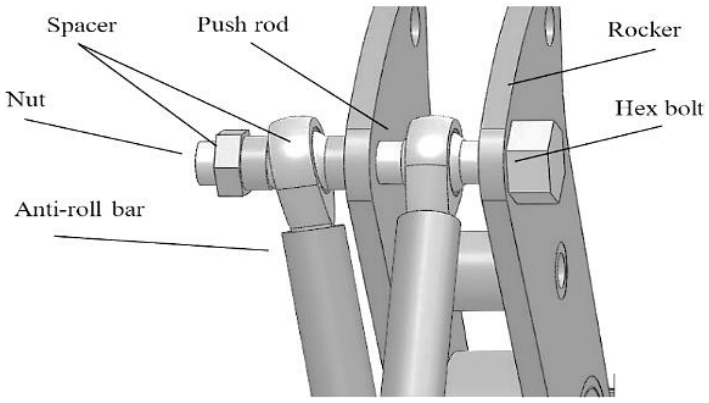

Fig. 5. Connection Rocker

Common hexagon bolts and matching nuts fix the rod ends to the arms and the rockers. The ARB rod ends will be connected to the same location on the rockers as the pushrod. The rod ends will be mounted on the outer side of the rocker and spacers will be placed on either side of the heim joints to ensure that sufficient clearance is available. The spacers could be manufactured out of a matching tube (Figure 5). The above designs recommend bolting the entire ARB system to the frame, which makes it removable. Making the roll bar removable simplifies servicing and allows for easy adjustments. Due to the stability of the frame, it is not recommended to bolt the ARB directly on the frame tubing. Therefore, additional saddles or metal sheets will have to be welded to the frame. This removes the chances of damaging the frame from the tension of the mounting bolts.

The most convenient and practical mounting point of the ARB system is underneath the frame and the floor closeout. This location ensures that functional components will not be interfered with, and the closeout works as a secure barrier for the driver. The distance between the lowest point of the ARB system and the ground is large enough to ensure that there will be no contact. This satisfies the FSAE rules for ground clearance. Another advantage of the above configuration is that as the front ARB is not located in the driver's cell, it does not require a cover (Driver's leg protection regulation).

2.3. Numerical analysis

2.3.1. Force and endurance limit calculation

To perform FEA on the anti-roll model, the applied force acting on the ARB and its endurance limit should be determined. From the free body diagram of the rocker shown in

Figure 6, which is obtained from a maximum cornering load case, the applied force acting on the ARB can be identified. It should be noted that the suspension rocker and spring had a direct influence on the anti-roll design. First, the geometry of the rockers determined the displacement of the ARB lever arms during suspension spring compression. Vertical displacement influenced the torsion in the bar while horizontal displacement (that is, in the plane of the rocker faces) influenced the stress experienced at the lower heim joints. Second, the suspension spring stiffness affects the degree of vehicle roll, which will be resisted by the springs through a parameter known as spring rate. The spring rate is the relationship between load and deflection. When used in conjunction with the ratio of wheel movement to spring movement, the total portion of vehicle roll that is resisted by springs can be calculated.

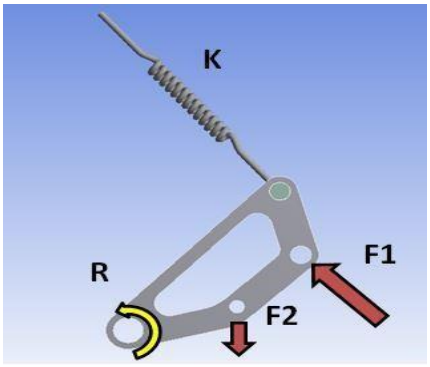

Fig. 6. Free body diagram of the rocker

Tab. 1

Endurance limit factors for the fatigue stress concentration

Factors	Description	Value	Reasoning or formula
C_a	Load factor	1.0	Using von Mises equivalent
C_b	Size factor	0.91	For rotating circular shaft: $C_b = 1.189 d^{-0.097} = 1.189(16) = 0.91$
C_c	Surface factor	0.78	For machined-cold drawn 4130 Chrome-Moly
C_d	Temperature factor	1.0	Assuming operating temperature $T < 350℃$
C_e	Reliability factor	0.814	Assuming 99% reliability
C_f	Stress concentration factor	0.868	Taking into consideration the added fillets on the moment arms to represent welds: $C_f = \frac{1}{1+q(kt-1)} = \frac{1}{1+0.(1.2-1)} = 0.868$
C_g	Miscellaneous effects factor	1.0	Assuming no other significant factors

The spring stiffness (K), maximum rotation (R), and F1 are 44 N/mm, 24°, and 2500 N. F2 is the unknown force acting on the ARB moment arm from the rocker mounting point. Breaking the load of 2500 N into X and Y components gives forces of 1767.76 N acting in both directions. Inputting the rotation and spring properties, an estimated worst-case value for F2 of

approximately 400 N was obtained using the force probe tool in ANSYS. F2 will apply an upward force on the ARB, causing a reaction force of 400 N to act on the opposite side of the ARB in a downward direction, creating torsion in the ARB. This loading will occur during cornering when the ARB acts to equalize loads between the left and right suspension systems. The loading will be fully reversed.

From Table 1 and Eq. 1, the fatigue stress concentration for fatigue analysis (K_f) is 0.5015; the fillet weld stress concentration was also accounted for through the endurance limit factors:

$$K_f = C_a C_b C_c C_d C_f C_g \tag{1}$$

2.3.2. Results and design development

Static structural analysis was set up and the geometry of the proposed ARB was imported directly from the SolidWorks model. The 4130 Chrome-Moly was chosen as the material of the ARB based on its availability, ease of manufacturing and desirable mechanical properties [6]. The initial model for FEA consisted of nine bonded bodies including four moment arm sheets, 16 mm diameter and 3 mm thick hollow torsion bar, two inserts and two bolts. However, to improve the model, the initial assembly was combined into one body to eliminate issues with the bonded contacts; the bolt was removed and replaced by a distributed load on the holes of either moment arm. To further increase the accuracy of the model in ANSYS and represent the welds that will be used to bond the lever arms to the shaft, 5 mm fillet welds were considered and added on either side of the lever arm plates. This is a conservative and practical value for the given application (Appendix A has details of the weld analysis). A solid fillet is stronger than an actual weld; however, this should help improve the accuracy of the model and can be considered in the endurance limit.

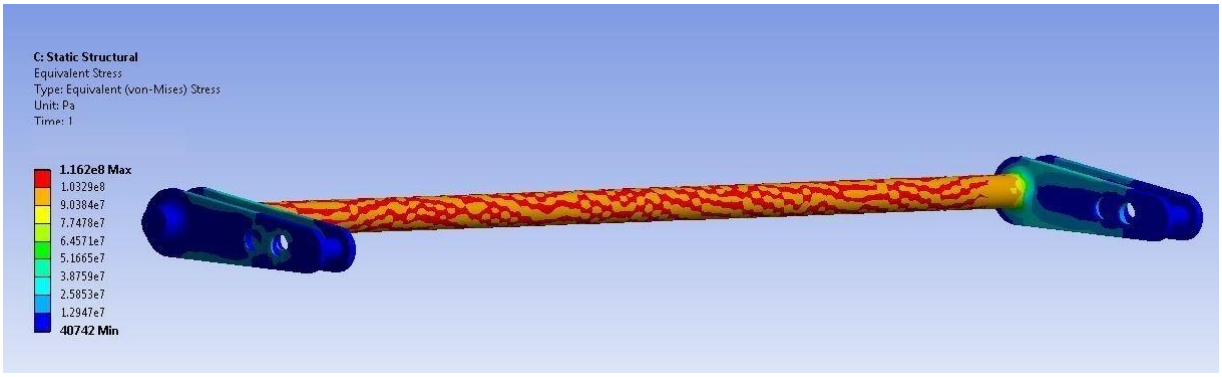

Fig. 7. Stress distribution from the first FEA

The first FEA result of the model is shown in Figure 7 above. The distribution of the stress throughout the shaft was evenly distributed; however, there is a relatively large maximum stress of 162.8 MPa occurring on the inside of the moment arms. In addition, Figure 8 shows the safety factor of 0.74185, which indicates failure. Therefore, to increase the factor of safety to above 1, design changes will be made to improve the strength of the ARB model.

Two changes were made, the length of the moment arms was shortened, reducing torsion on the bar and the torsion bar was changed from a hollow 3 mm tube to a solid bar. These changes, however, have some negative effects, as changing the length of the moment arms reduces the amount of adjustability available to the vehicle. Likewise, changing the torsion bar from tubular to solid will increase the cost and overall weight of the ARB. However, both of these changes will increase the overall stiffness and strength of the ARB. Note that the adjustment of the outside diameter of the ARB tube was also a possible option. However, an increase in the outer diameter would have the effect of increasing the torsional stiffness and, subsequently, the shear stress. Greater torsional stiffness decreases angular deflection, meaning that a larger portion of one lever arm displacement is transferred to the opposite lever arm. This has the effect of increasing vehicle roll resistance.

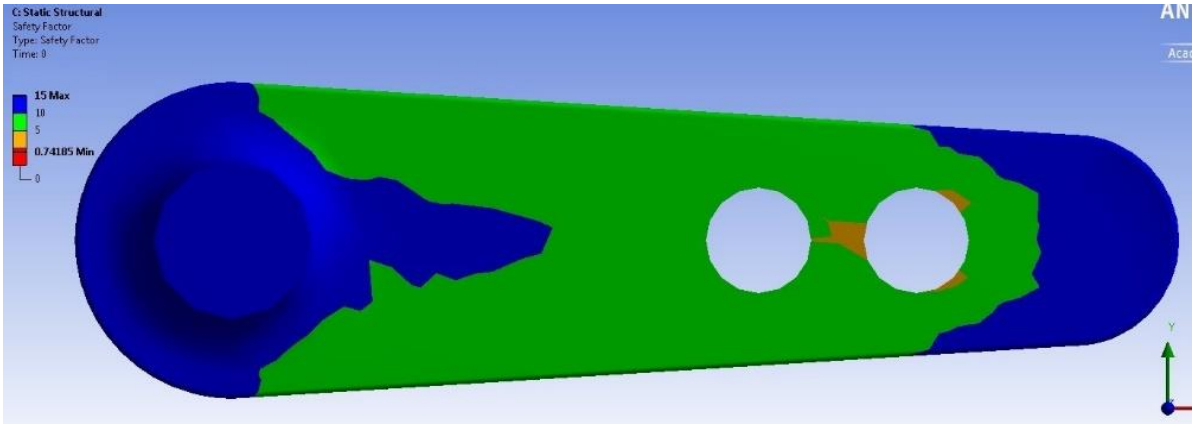

Fig. 8. Initial model for FEA analysis

The moment arms were reduced to a length of 65 mm centre to centre rather than 80 mm. This reduces the moment acting on the bar. Along with the solid Chrome-Moly bar, this reduced the maximum stress to 81.55 Mpa. The maximum and minimum stresses obtained from the second FEA are shown in Figure 9. Similarly, the minimum and maximum strain occur in the same locations of the maximum and minimum stress; the maximum value for strain is 0.00039821 m/m. From Figure 10, the maximum deformation in the ARB is 0.0013871 m. This occurs between the ends of the two moment arm sheets as expected, as the moment rotates around the ARB from this point. The safety factor obtained, as shown in Figure 11, had a value of 1.057 minimum, which gives infinite life to the entire ARB. Therefore, the recommended solutions are altering the ARB to a solid Chrome-Moly bar and shortening the moment arms from 80 to 65 mm. In addition, the previously used inserts, which supported the welding of the arm plates to the torsion bar, are now unnecessary. The final anti-roll design is shown in Figure 12.

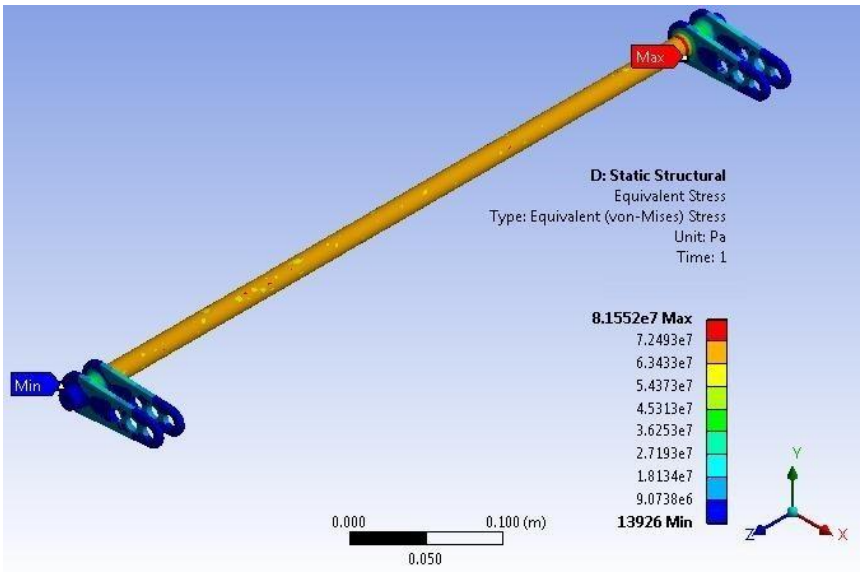

Fig. 9. Stress distribution from the second FEA

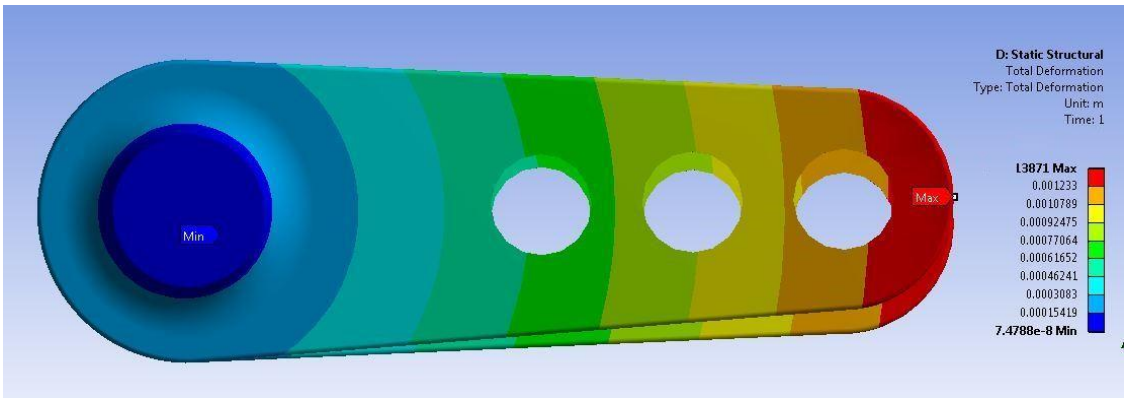

Fig. 10. Deformation from the second FEA

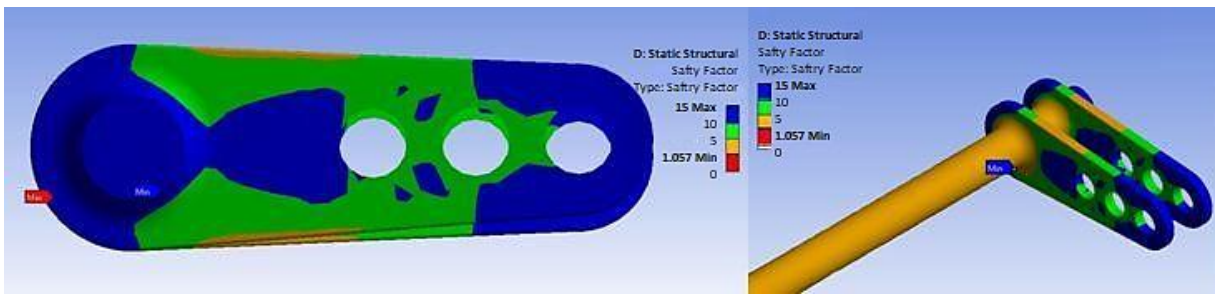

Fig. 11. Safety factor from the second FEA

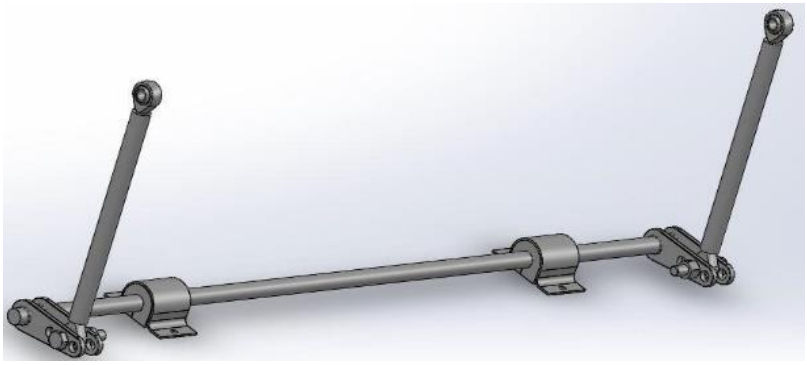

Fig. 12. Final design

2.4. Design assessment

While the FEA analysis determined the required dimensions to avoid failure, the following section partially assesses the effectiveness of the ARB design in providing roll resistance. For a solid rod subject to torsion, the following equations from reference [7] are used to calculate the angular deflection, spring rate and factor of safety of the bar. These parameters are typically used in the calculations for the required diameter of ARBs to achieve a specified roll resistance.

2.4.1. Angular deflection

The bar is assumed to be constructed from 4130 Chrome-Moly, which has a yield strength S_y of 435 MPa, modulus of elasticity E of 205 GPa and a Poisson's ratio ν of 0.29. The force of 400 N applied 65 mm from the bar resulted in a torsion T of 26 Nm. The lengths L of the front and rear torsion bars are 736 and 600 mm, respectively. Both bars have a diameter d of 16 mm. The angular deflection is [7]:

$$\theta = \frac{64TL\left(1+\nu\right)}{\pi d^4 E} \tag{2}$$

The above analysis resulted in an angular deflection of 34.31 and 27.97° for the front and rear, respectively. The angular deflection is the amount of twist over the length of the bar and was used in ref [3] to determine the roll motion ratio of the vehicle. The roll motion ratio was then used in combination with the body roll angle and the vehicle roll resistance to determine the required diameter of the bar. This parameter is used as an indication of the effectiveness of the current design. Using the maximum target body roll angle (ϕ) of 1.5°/g [5] in a 1.2 g corner and the equation $roll\ motion = \theta / \phi$ [3].

The estimated roll motion ratios for the front and rear are 19.06 and 15.4 compared with the result of ref [3] with a roll motion ratio of 10.7, meaning that the current design has a 'softer' ARB and provides less roll resistance to the vehicle. The spring rate or the torsional resistance of the bar may also be compared using the following equation [7]:

$$K = \frac{\pi d^4 E}{64L\left(1+\nu\right)} \tag{3}$$

2.4.2. Spring rate

The amount of the vehicle roll that is resisted by the suspension system is calculated using the spring rate. The spring rate is the ratio of wheel movement to spring movement. The spring rate K was found to be 852.05 Nm/rad, which is comparable to the results of ref [3] 1000 Nm/rad. URE's ARB system is more 'hard' as it has greater torsional resistance and translates more of the force between the left and right suspension systems.

2.4.3. Safety factor

Safety factor is determined using the following equation [7]:

$$N = \frac{\pi d^3 S_y}{16T\sqrt{3}} \tag{4}$$

The factor of safety for the front and rear solid ARB rods using static loading conditions was found to be 7.768. This indicates that the bar is highly unlikely to fail. Under fatigue loading, the factor of safety would be reduced; however, given the safety margin, it is not expected to fail. In ref [3], was reported a static safety factor of 1.4 for the front ARB. As they completed a full analysis with measured data and vehicle dynamics simulations, their need to be conservative was significantly less, so the safety factors are comparatively different.

3. CONCLUSION

This paper provides key considerations for designing and analysing the ARB system of a Formula SAE vehicle produced by James Cook University students. There are several recommendations and outcomes for the design of an actual ARB. The connection between the lever arms and the bar, the geometry of the lever arms and the connection of the entire ARB system to the frame are clearly discussed. Furthermore, the geometry of the rockers is shown as the proper option to determine the displacement of the lever arms during suspension spring compression and related forces. By considering welding requirements, weight and strength, the Chromoly was an appropriate option for the design. Thus, it is proposed that the geometry of rockers is highly influential on the function of the bar. To ensure the quality, the proposed system is designed based on the FSAE rules, and the justification is achieved through finite element analysis by investigating the stress and strain of each part of the system and the safety factor using SolidWorks and ANSYS. The design assessment is performed by comparing some important parameters including the angular deflection, spring rate and factor of safety of the bar with the corresponding values taken from the literature.

APPENDIX A

This analysis was used to determine the size of the fillet welds located on either side of the four lever arm plates. Figure 13 shows the force F applied by the drop link connection and the reaction force V and moment T about the torsion bar axis. The external force used in the FEA analysis was 400 N. The applied force will therefore be 200 N for a single lever arm plate. The furthest adjustment setting L imposes maximum stress, so is used as a critical load

case. The external force is applied in-plane and offset from the centroid of the weld group G, subjecting it to direct shear stress (primary τ') and superimposed torsional stress (secondary τ"). The force vectors of the primary and secondary shear are also shown in Figure 13. The dimensions of the bar used in the analyses are L=65 mm and r=8 mm.

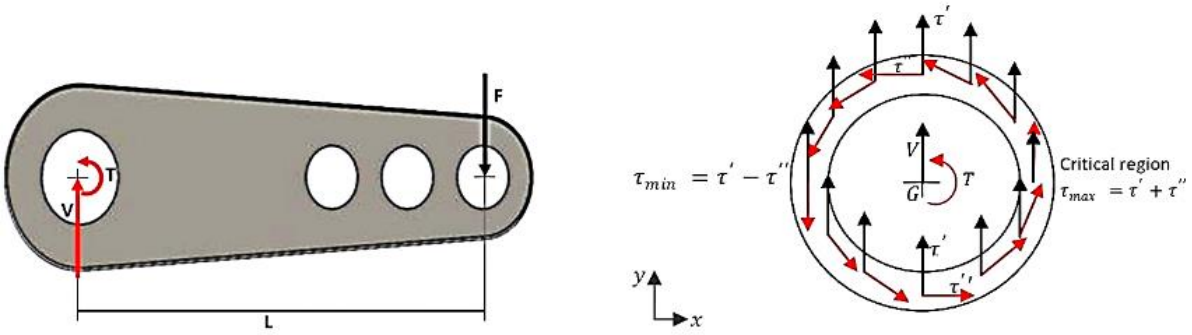

Fig. 13. Lever arm free body diagram and weld group

From Figure 13, the maximum stress will be on the inner side of the ARB if the external force is down (shown), and on the outside, if the external force is up. As the throat length t of the fillet weld is unknown, the unit polar moment of inertia J is used in the calculations.

The weld group will be subject to fully reversed cyclic loading, approximated using a sine curve and analyzed on an SN diagram. The endurance limit, S_e assumes the weld rod is ER80-D2, which has an ultimate tensile strength of 80 ksi, reliability of 99% and the weld 'reinforcement' is present. The welds are compared to the Goodman failure criteria for infinite life ($S_{FN}=S_e$) with a safety factor N of 1.5. The following analysis uses equations from ref [7]. Total torsional stress:

$$\tau = \tau' + \tau'',\ \tau' = \frac{V}{A} = \frac{V}{1.414\pi hr},\quad \tau'' = \frac{Tr}{tJ} = \frac{V}{1.414\pi hr^2} \tag{5}$$

Where V, T, A, r, h, t and J are shear force, twisting moment, cross-sectional area of the rod, radius of the rod, the weld size, thickness of the rod and moment of inertia, respectively. Equivalent von Mises stress ($\sigma = \sqrt{3}\tau,\ \sigma'_{max} = \sqrt{3}\tau,\ \sigma'_{min} = -\sqrt{3}\tau,\ \sigma'_m = 0,\ \sigma'_a = \sqrt{3}\tau$). σ'_{max} , , $'_{min}$ and σ'_m are maximum, minimum and mean stress, respectively, and σ'_a is stress amplitude. Endurance strength$(S_e = S_e' C_a C_b C_c C_d C_f C_g)$ where S_e' is the ideal endurance strength $S_e' = 0.5 S_{ut} = 275.79\ MPa$ and endurance limit factors are proposed in Table 2. From the above equations, S_e is 31.231 MPa.

From the above analysis, the recommended leg size of the weld is 0.02 mm. This small value indicates that the estimated maximum loading conditions will not damage the integrity of a 5 mm weld (Table 3).

Tab. 2

Endurance limit factors for the fatigue stress concentration

Factors	Description	Value	Reasoning
C_a	load factor	1.0	Using von Mises equivalent
C_b	Size factor	0.8	Convention
C_c	Surface factor	0.47	Weld with reinforcement attached, assume equivalent to 'As forged'
C_d	Temperature factor	1.0	Assuming operating temperature $T < 350℃$
C_e	Reliability factor	0.814	Assuming 99% reliability
C_f	Stress concentration factor	0.37	$C_f = 1/K_f$, Assuming that the fatigue stress concentration factor is equivalent to the toe of a fillet weld subjected to transverse loading, $K_f = 2.7$ [7]
C_g	Miscellaneous effects factor	1.0	Assuming no other significant factors

Tab. 3

Endurance limit factors for the fatigue stress concentration

Variable	Description	value
V	Shear force	200 N
A	Cross-sectional area of the rod	0.0335 h
T	Twisting moment	13 Nm
τ'	Primary shear stress	5627.826 h^{-1}
τ''	Secondary shear stress	45726 h^{-1}
$\sigma_m^{'}$	Mean stress	392.507 h^{-1}
S_e	Endurance limit	31.231 MPa

Reference

1. Staniforth Allan. 2006. *Competition Car Suspension*. Haynes Publishing. ISBN: 978-1844253289.
2. Milliken William, Milliken Douglas. 1995. *Race Car Vehicle Dynamics.* SAE International.
3. Bos Van Den. 2010. „Design of a Formula Student Race Car Spring-Damper System". *PhD thesis*. Eindhoven University of Technology. Department of Mechanical Engineering.
4. *Formula SAE Rules*. 2015. SAE International.
5. Gould Daniel. 2006. "Lateral weight transfer and roll resistance". In: *Competition Car suspension*. Haynes Publishing.
6. MatWeb. "AISI 4130 Steel Normalised at 870 deg". Available at: http://www.matweb.com/search/DataSheet.aspx?MatGUID=e1ccebe90cf94502b35c2a4745f63593&ckck=1.

7. Juvinall Robert C., Kurt M. Marshek. 2006. *Fundementals of Machine Component Design*. Technology & Engineering.

Received 10.04.2022; accepted in revised form 02.06.2022

Scientific Journal of Silesian University of Technology. Series Transport is licensed under a Creative Commons Attribution 4.0 International License